Turbulence and standing waves in oscillatory chemical reactions with global coupling

Cite as: J. Chem. Phys. **101**, 9903 (1994); https://doi.org/10.1063/1.468482
Submitted: 16 May 1994 • Accepted: 10 August 1994 • Published Online: 31 August 1998

Florian Mertens, Ronald Imbihl and Alexander Mikhailov

Turbulence and standing waves in oscillatory chemical reactions with global coupling

Florian Mertens and Ronald Imbihl
Fritz-Haber-Institut der Max-Planck-Gesellschaft, Faradayweg 4-6, D-14195 Berlin (Dahlem), Germany

Alexander Mikhailov
Fritz-Haber-Institut der Max-Planck-Gesellschaft, Faradayweg 4-6, D-14195 Berlin (Dahlem), Germany and N. N. Semenov Institute for Chemical Physics, Russian Academy of Sciences, ul. Kosygina 4, 117333 Moscow, Russia

(Received 16 May 1994; accepted 10 August 1994)

Using the model of the complex Ginzburg–Landau equation with global coupling, the influence of long-range interactions on the turbulent state of oscillatory reaction–diffusion systems is investigated. Experimental realizations of such a system are, e.g., oscillatory reactions on single crystal surfaces where some of the phenomena we simulate have been observed experimentally. We find that strong global coupling suppresses turbulence by transforming it into a pattern of standing waves or into uniform oscillations. Weaker global coupling gives rise to an intermittent turbulent state which retains partial synchrony. © *American Institute of Physics.*

Oscillatory surface reactions demonstrate a large variety of spatiotemporal patterns, both regular and chaotic.[1–3] Spatial coupling in these reactions under isothermal conditions is provided by two basic mechanisms: surface diffusion of mobile adsorbates on the catalyst surface and changes of the educt pressures in the gas phase. The latter arise due to the mass balance in the reaction and, since mixing in the gas phase is very fast, this coupling is global. Gas-phase coupling is known to significantly influence the course of oscillatory surface chemical reactions by tending to synchronize the oscillations.[4–5] Under certain conditions, periodically oscillating patterns of standing waves have been found on the surfaces.[4]

To consider the effects of global coupling in oscillatory reaction–diffusion systems, we have proposed a simple mathematical model obtained by including an additional global coupling term into the complex Ginzburg–Landau equation (CGLE).[6,7] Although such a model can be fully justified only in the vicinity of a Hopf bifurcation, its analysis also reveals more general qualitative properties of the involved phenomena and thus provides a basis for the interpretation of experimental data. Using this model, we have investigated the breakdown of synchronization caused by strong supercritical inhomogeneities (surface defects), we studied propagation of phase flips over the globally synchronized state and the spontaneous formation of large-scale oscillation domains.[6,7] This analysis has been performed in a parameter region where diffusional coupling between oscillators tends to synchronize the local oscillations.

However, depending on the dynamical properties of oscillations in the individual surface elements and on the ratio of surface diffusion constants for different adsorbed reagents, local diffusional coupling may also destabilize uniform bulk oscillations and give rise to chaotic spatiotemporal regimes known as chemical turbulence.[8,9] Under proper choice of the parameters, these turbulent regimes can be described by the CGLE. A detailed statistical analysis of turbulence in CGLE, based on its numerical simulations, has been carried out in Refs. 10–13.

The purpose of the present paper is to investigate how the effect of global coupling, which is common to all oscillatory surface reactions, changes the properties of diffusion-induced chemical turbulence. By varying the relative intensity of the additional global coupling term in CGLE, a transition from uniform synchronous oscillations (for a very strong global coupling) to periodic standing waves and further to a turbulent state (for a weaker coupling) is found as shown below. The analysis of the turbulent state, realized in the presence of global coupling, shows that its properties are qualitatively different from those of diffusion-induced turbulence realized in absence of global coupling. It retains a certain degree of long-range order and its temporal behavior can be characterized as *intermittent*, i.e., turbulent bursts appear on the background of almost synchronous oscillations. Based on the results of our analysis we attempt a qualitative comparison with experimental observations.

Our mathematical model consists of a dynamical equation for the local complex oscillation amplitude $\eta(\mathbf{x},t)$ in a population of small-amplitude limit-cycle oscillators which are coupled both locally and globally. By choosing appropriate dimensionless units, it can be written in the form[6]

$$\dot{\eta}=(1-i\omega)\eta-(1+i\beta)|\eta|^2\eta+(1+i\epsilon)\nabla^2\eta-\mu e^{i\chi}\bar{\eta}, \quad (1)$$

where

$$\bar{\eta}=(1/S)\int d\mathbf{x}\eta(\mathbf{x},t) \quad (2)$$

is the spatial (surface) average of the local oscillation amplitudes (S is the total surface area). It differs from the standard CGLE[14] by the last integral term in Eq. (1) which can be interpreted as a driving force applied to each individual oscillator and collectively produced by all oscillators in the population. The intensity of global coupling is characterized by the coefficient μ, the factor with χ in the last term takes into account a possible phase shift between the driving force and the averaged amplitude $\bar{\eta}$. The Benjamin–Feir (BF) instability leading to diffusion-induced turbulence occurs for Eq. (1) without global coupling ($\mu=0$) if the condition

$1+\epsilon\beta<0$ holds. Below, in contrast to our previous publications,[6,7] we consider the parameter region where this condition is satisfied.

The local phase ϕ and (real) amplitude ρ of the oscillations can be introduced by

$$\eta(\mathbf{x},t)=\rho(\mathbf{x},t)\exp[-i\Omega t-i\phi(\mathbf{x},t)], \tag{3}$$

where $\Omega=\omega+\beta+\mu(\sin\chi-\beta\cos\chi)$. Substituting Eq. (3) into Eq. (1), two coupled dynamical equations for the variables $\rho(\mathbf{x},t)$ and $\phi(\mathbf{x},t)$ are obtained:

$$\dot{\rho}=(1-\rho^2)\rho-\nabla^2\rho-\rho(\nabla\phi)^2+\epsilon\rho\nabla^2\phi+2\epsilon\nabla\rho\nabla\phi - \mu R\cos(\phi-\Psi+\chi), \tag{4}$$

$$\dot{\phi}=\omega+\beta\rho^2-\Omega+(2/\rho)\nabla\rho\nabla\phi+\nabla^2\phi-(\epsilon/\rho)\nabla^2\rho + \epsilon(\nabla\phi)^2+(\mu R/\rho)\sin(\phi-\Psi+\chi). \tag{5}$$

The global phase Ψ and amplitude R are determined by

$$R\exp[-i\Psi(t)]=(1/S)\int d\mathbf{x}\,\rho(\mathbf{x},t)\exp[-i\phi(\mathbf{x},t)]. \tag{6}$$

The uniform bulk oscillations with frequency Ω correspond to the steady state of Eqs. (5) and (6) with $\phi(\mathbf{x},t)=\Psi=\phi_0$ and amplitude $\rho(\mathbf{x},t)=R=\rho_0=(1-\mu\cos\chi)^{1/2}$.

To investigate the stability of this steady state we take $\rho(\mathbf{x},t)=\rho_0+\delta\rho(x,t))$ and $\phi(x,t)=\phi_0+\delta\phi(x,t)$ and linearize Eqs. (4) and (5) with respect to small perturbations $\delta\rho$ and $\delta\phi$. The solution of the linearized equations is given by a sum of independent spatial modes. If the system is one dimensional and we have no-flux boundary conditions at $x=0$ and $x=L$, these modes are

$$\delta\rho(x,t)=\delta\rho_k\exp(\gamma_k t)\cos(kx), \tag{7}$$

$$\delta\phi(x,t)=\delta\phi_k\exp(\gamma_k t)\cos(kx), \tag{8}$$

where $k=2\pi n/L$, $n=1, 2,...$ The rate γ_k of growth (or decay) of the mode with the wave number k satisfies

$$(\gamma_k+2\rho_0^2+k^2)(\gamma_k-\mu\cos\chi+k^2) +(\epsilon k^2-\mu\sin\chi)(2\beta\rho_0^2+\epsilon k^2-\mu\sin\chi)=0. \tag{9}$$

When $\mu/\epsilon\ll k^2\ll 1$ it has an approximate solution

$$\gamma_k=\mu(\cos\chi+\beta\sin\chi)-(1+\epsilon\beta)k^2 -(\epsilon^2/2)(1+\beta^2)k^4. \tag{10}$$

Hence, the behavior of these modes is determined by the signs of the combinations $q=\cos\chi+\beta\sin\chi$ and $b=1+\epsilon\beta$. As mentioned above, the case $b>0$ was considered by us in the previous publications;[6,7] it corresponds to diffusion-induced synchronization. When $q>0$, global coupling provides a positive feedback and induces its own breakdown.[7] In the present paper we investigate the behavior of the system under the conditions that $q<0$ and $b<0$.

In the case considered here, the rate γ_k is maximal for the mode with the wave number $k=k_0$ given by

$$k_0^2=\frac{2|1+\epsilon\beta|}{\epsilon^2(1+\beta^2)}. \tag{11}$$

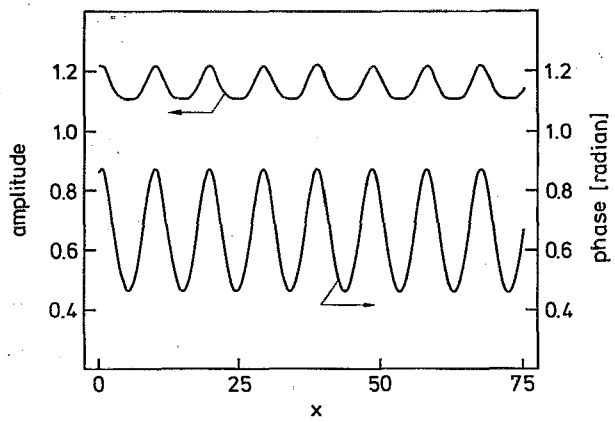

FIG. 1. Profiles of the amplitude and the phase in a standing wave obtained by numerical simulation of Eq. (1) with parameter values $\beta=-1.5$, $\epsilon=2.0$, $\chi=\pi$, and $\mu=0.33$; the total length of the system is $L=256$.

The mode with this wave number is growing ($\gamma_k>0$) only if $\mu<\mu_0$ where

$$\mu_0=\frac{(1+\epsilon\beta)^2}{2q\epsilon^2(1+\beta^2)}. \tag{12}$$

Hence, we find that strong enough global coupling ($\mu>\mu_0$) stabilizes uniform synchronous oscillations and thus suppresses the diffusion-induced instability. When the intensity of global coupling is decreased, uniform oscillations at $\mu=\mu_0$ become unstable in respect to growth of standing waves with the wave number $k=k_0$.

To determine the nonlinear evolution of growing modes we performed one-dimensional numerical simulations of Eq. (1). They show (Fig. 1) that the bifurcation is supercritical and for $\mu<\mu_0$ near the threshold we have stationary standing waves of a small amplitude.

The standing waves which are established in the system as a result of such an instability have several characteristic features. The amplitude of the local oscillations in the nodes of such waves does not vanish; therefore they can be also considered as a superposition of a small-amplitude standing wave and spatially uniform oscillations. Moreover, the phase of oscillations is also periodically spatially modulated in such a standing pattern and reaches its minima in the nodes where the oscillation amplitude is minimal.

The phenomena leading to the formation of standing waves can be interpreted as a *self-resonance* in the system considered. Similar resonance effects are found in the presence of external periodic forcing applied to oscillatory distributed systems.[15] It should be emphasized that the lowest-order resonance (with $n=1$ in notations of Ref. 15) is responsible for formation of standing waves in our system. In the analysis of standing waves for CO oxidation performed earlier in Ref. 16 the effect was attributed to a higher-order self-resonance ($n=2$) with the consequence that it could occur only under very special conditions of the codimension-two bifurcation. In the framework of our model such higher self-resonance would be described by the terms proportional to $\bar{\eta}^2\eta^*$ in Eq. (1). We do not include such

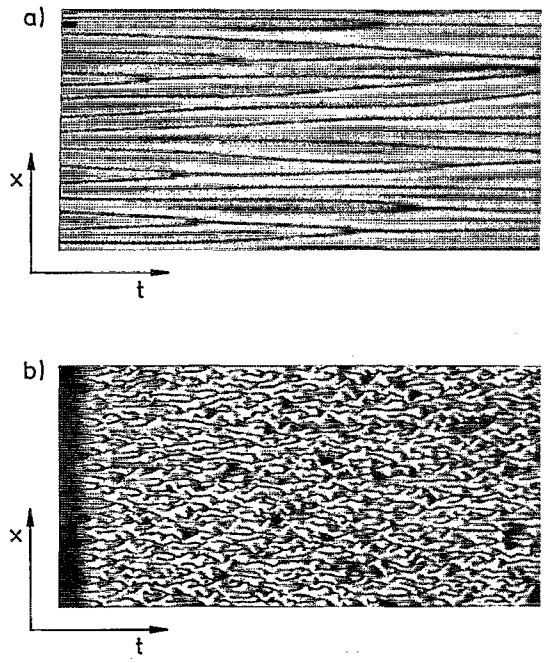

FIG. 2. Different turbulent regimes in CGLE without global coupling. (a) Phase turbulence ($\beta=-1$, $\epsilon=1.5$, $L=256$, the integration interval shown is $T=200$). (b) Defect turbulence ($\beta=-2$, $\epsilon=2$, $L=256$, $T=200$, the initial state is uniform with small random perturbations). The time development of the local real amplitude $\rho(x,t)=|\eta(x,t)|$ of oscillations is shown in gray scale, with darker areas corresponding to larger values of ρ. The defects are seen in (b) as moving white spots.

terms and do not explicitly consider their effect because, for small amplitudes η, their magnitude is small in comparison to the leading linear term, proportional to $\bar{\eta}$ in Eq. (1).

When the intensity of global coupling is further decreased, the stationary pattern of standing waves is destroyed, and spatiotemporal chaos appears. For $\mu=0$ the system is described by CGLE without global coupling which was investigated in Refs. 8,10–13. At this stage the system can be found, depending on the proximity to the boundary $b=0$ of the BF instability, either in the state of phase turbulence [Fig. 2(a)] or in the state of amplitude turbulence [Fig. 2(b)].

Phase turbulence is characterized by random motion of *shocks* representing narrow regions with an increased oscillation amplitude. The statistical analysis shows that this disordered state has long-range correlations and oscillations of distance elements are almost synchronous.[12]

On the other hand, amplitude turbulence demonstrates a large number of dynamical defects which represent (in the one-dimensional case) narrow regions where the local oscillation amplitude almost vanishes.[17] This highly chaotic state has only short-range spatial correlations, i.e., the oscillations of different elements are desynchronized.[12]

We have numerically investigated a transition towards fully developed (phase or amplitude) turbulence which takes place as the magnitude of the global coupling coefficient is gradually decreased. The periodic stationary pattern of standing waves persists within an interval of μ below the destabilization threshold of the uniform state. The profile of standing waves changes with a decrease of μ and becomes

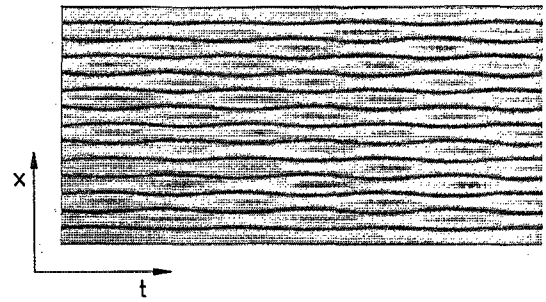

FIG. 3. Breathing standing waves at $\mu=0.02$ for $\beta=-1.0$, $\epsilon=1.5$, $\chi=\pi$, $L=256$, and $T=800$; local values of the real oscillation amplitude are shown in gray scale.

strongly unharmonical (Fig. 1). The real amplitude ρ is then almost flat, except for narrow intervals (i.e., shocks) where it is a little larger. Inside the shocks the oscillation phase ϕ is also slightly increased.

When a certain critical value of the global coupling coefficient μ is reached, these stationary standing waves become unstable and are replaced by a breathing periodic pattern where the shocks perform periodic oscillations around their equilibrium positions (Fig. 3). The amplitude of such oscillations grows when μ is decreased. When the oscillation amplitude of the shocks becomes close to the spatial period of the pattern, the pattern loses its regularity. Collisions between the shocks result in their mutual annihilation and new shocks are occasionally produced between the existing ones. This stage is very similar to phase turbulence in absence of global coupling [cf. Fig. 2(a)]. Note that the average oscillation amplitude $|\bar{\eta}|$ in this turbulent state is only a little

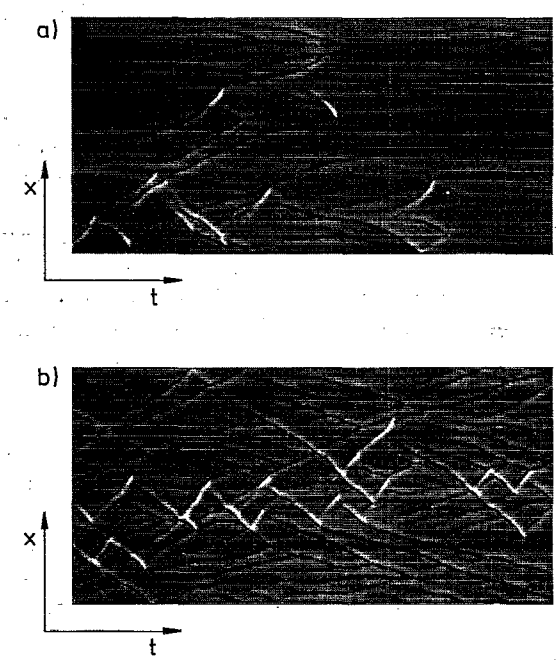

FIG. 4. Spontaneous formation of defects (white regions) on the background of phase turbulence in the presence [(a) $\mu=0.0505$] and in absence [(b) $\mu=0$] of global coupling; other parameters are $\beta=-1.0$, $\epsilon=2.0$, $\chi=\pi$, $L=256$, $T=400$. Local values of the real oscillation amplitude ρ are shown in gray scale.

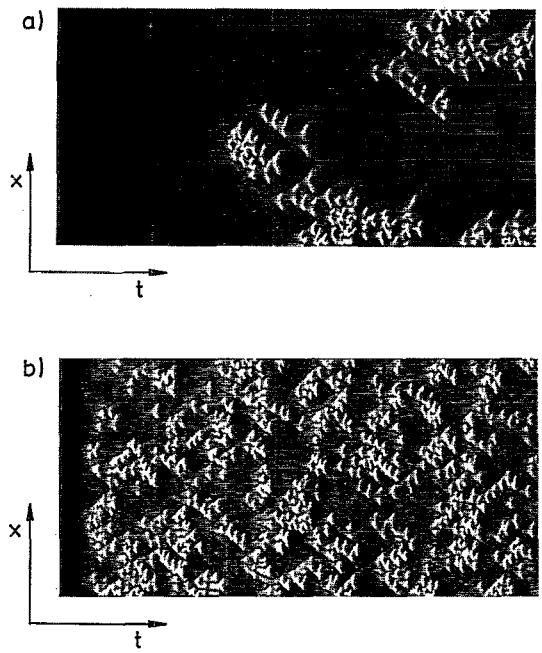

FIG. 5. Intermittent turbulent regimes in the presence of global coupling: (a) at $\mu=0.3$ for $\beta=-1.5$ and (b) at $\mu=0.5$ for $\beta=-2.0$; other parameters are $\epsilon=2.0$, $\chi=\pi$, $L=256$, and $T=400$. Local values of the real oscillation amplitude ρ are shown in gray scale.

smaller than for the uniform oscillations. It means that oscillations remain almost synchronous in this case. Phase turbulence is the terminal state of the system (at $\mu=0$) close enough to the boundary $b=0$ of the BF instability.

Farther from the BF boundary the phase turbulence is only a transient stage of the system's evolution. Here the numerical simulations show the spontaneous creation of defects [Fig. 4(a)]. Some of the shocks start suddenly to accelerate, run into their neighbors, and thus produce small areas where the oscillation amplitude almost vanishes, i.e., amplitude defects. This process is similar to the transition to the amplitude turbulence in CGLE without global coupling [Fig. 4(b)].

Although the properties of individual amplitude defects are not apparently modified by the presence of global coupling, their collective behavior is different. They tend to form compact groups which have finite lifetimes. Figure 5(a) shows that local bursts of the amplitude turbulence are surrounded by larger "laminar" regions filled by periodic standing waves. Such a turbulent state can be characterized as *intermittent*. When the intensity of global coupling is smaller [Fig. 5(b)] the bursts become more frequent and the state of the medium between them approaches that of the phase turbulence. However, it is still significantly different from the developed amplitude turbulence without global coupling [cf. Fig. 2(b) for the same values of the system parameters but $\mu=0$].

The intermittency which persists in the presence of global coupling is qualitatively different from the one recently found in Ref. 18 in a narrow parameter region in two-dimensional simulations of CGLE without global coupling. In the latter case the defects multiplied until they filled the

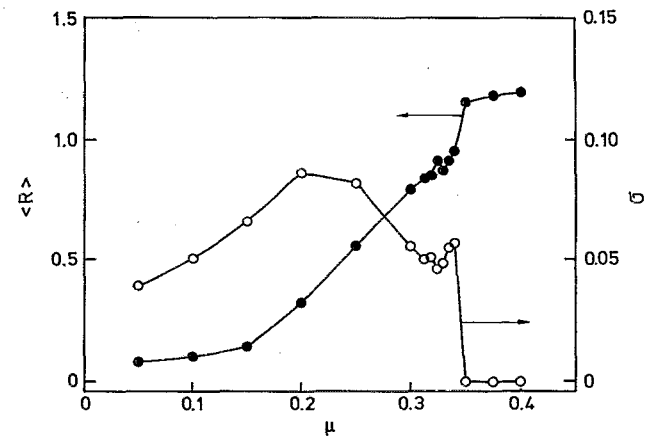

FIG. 6. Dependence of the time-averaged global oscillation amplitude (black circles) and its standard deviation (white circles) on the global coupling coefficient μ for $\beta=-1.5$, $\epsilon=2.0$, $\chi=\pi$, and $L=1024$.

entire medium. After that they became eventually suppressed by one spiral wave that gained control over the whole medium. In contrast to this, Fig. 5 shows well-localized bursts of defects. The intermittency which we have observed can be described as spontaneous random nucleation of the amplitude turbulence on the background of either regular standing waves or of phase turbulence. The appearing nuclei first grow but then die out.

A very interesting property of such intermittent turbulent regimes is that they do not lead to the synchronization breakdown, in contrast to the complete destruction of the synchronization by periodic waves emitted by emerging pacemakers which we have earlier described.[6,7] The absolute value $R(t)=|\bar{\eta}(t)|$ of the spatially averaged local oscillation amplitude $\eta(\mathbf{x},t)$ fluctuates with time in such an intermittent state around a stationary level. Figure 6 shows the calculated time-averaged value $\langle R\rangle$ of this amplitude (black circles) as a function of the global coupling coefficient μ and the standard deviation of the same quantity (white circles). For $\mu>0.34$ a

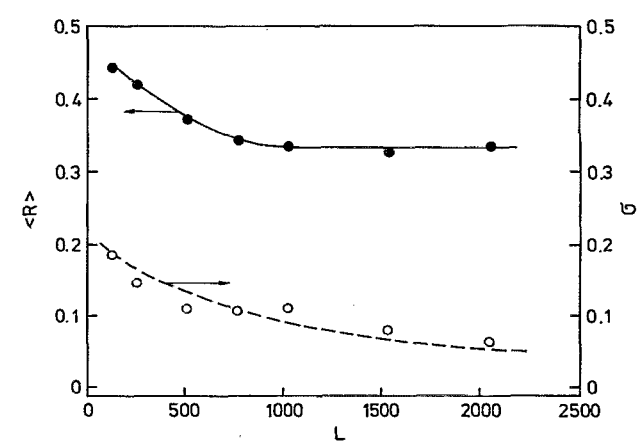

FIG. 7. Dependence of the time-averaged global amplitude (black circles) and its standard deviation (white circles) on the system size L at $\mu=0.2$, $\beta=-1.5$, $\chi=\pi$, and $\epsilon=2.0$; the averaging interval is $\Delta t=1600$.

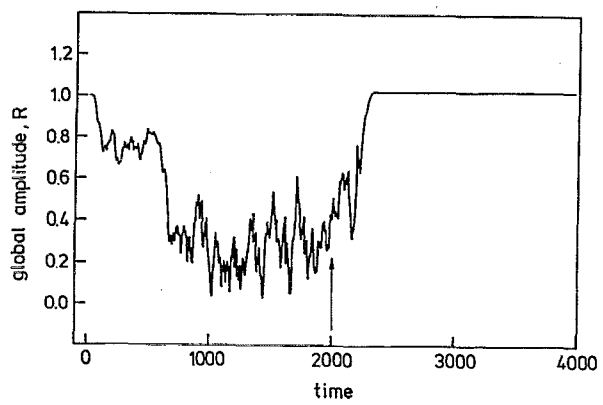

FIG. 8. Suppression of the defect turbulence by global coupling. In the time interval $0<t<2000$ the global coupling is absent ($\mu=0$) and, after an induction period, the system evolves into the state of the defect turbulence with almost vanishing average oscillation amplitude R. At time moment $t=2000$, shown by the arrow, global coupling with $\mu=0.07$ and $\chi=\pi$ is switched on which results, after a transient, in establishing of uniform synchronous oscillations.

coherent pattern (uniform oscillations or standing waves) is found in the system and therefore the standard deviation is close to zero. For smaller values of μ the intermittent amplitude turbulence develops and the local bursts of defects appear. The time-averaged amplitude R is considerably larger in this regime due to the contribution from the regions where standing waves or phase turbulence are still found.

Since we have performed our simulations for finite one-dimensional systems, a question is whether the intermittency effect is size dependent. Figure 7 shows the computed dependence of the mean value of R and of its standard deviation as functions of the total system's length L. We see that, although for smaller L some size effects are present, the dependence approximately saturates for larger systems so that the mean values are no longer size dependent (remaining small variations are the effect of the finite averaging time) while the standard deviation progressively decreases.

A phenomenon closely related to the continuous nature of the transition to turbulence is the absence of hysteresis. In the numerical experiment shown in Fig. 8 we have started our simulation from initial conditions representing uniform oscillations with small random perturbation without global coupling ($\mu=0$). After about 500 time units the defects spontaneously appeared and a state of amplitude turbulence has been established. This is seen in the significant reduction of the average oscillation amplitude R in Fig. 8. At a later time moment, shown by the arrow of Fig. 8, we switched on global coupling and followed the evolution of the system from the turbulent state into a complete recovery of uniform synchronous oscillations.

Although the main part of our numerical experiments has been performed for one-dimensional systems, we have also carried out a few two-dimensional simulations. They demonstrated a similar pattern of transition to turbulence upon a decrease of the global coupling intensity. The essential difference was that, instead of horizontal stripes which would have been a direct analog of standing waves in one dimension, we saw oscillatory standing wave patterns of hexagonal cells. When we started our simulations from random initial conditions, the array of cells was highly irregular, giving the impression of a foamlike structure with local hexagonal order. Moreover, the transition to defect turbulence was strongly facilitated and purely laminar states with only standing waves or phase turbulence were not yet obtained in our simulations.

In a single-crystal experiment in which the catalytic CO oxidation was studied on a Pt(110) surface, spatially resolved measurements revealed the existence of a standing wave concentration pattern on the catalyst.[4] These standing wave patterns appeared only in a very narrow region of the parameter space. Since the medium in this experiment is oscillatory and since the partial pressure variations in the gas phase provide a global coupling, one might consider these concentration patterns as the experimental counterpart of the standing wave patterns discussed here. Although the principal mechanism might be identical, one also has to be aware of some substantial differences between theory and experiment. Due to the geometry of the substrate lattice the surface diffusion on Pt(110) is strongly anisotropic thus favoring an effectively one-dimensional behavior which was seen in the experiment.[4]

A transition from synchronized oscillations to turbulence has been observed in the $NO+NH_3$ reaction on Pt(100).[19] The turbulent state in this reaction emerges as the strength of gas-phase coupling weakens with decreasing temperature. This finally leads to the complete breakdown of the rate oscillations (the amplitude of which corresponds in our model to $\bar{\eta}$). Before the complete breakdown of global coupling takes place one observes the coexistence of localized patterns such as spiral waves with areas still oscillating in a synchronous manner. The situation is quite similar to that of Fig. 5 where we have the coexistence of defects with synchronized behavior. There is of course also one important difference since in the experiment the spirals are typically pinned to structural defects of the surface while in the simulations we assume a homogeneous medium.

Finally, we note that, due to great simplicity and generality of the considered model of CGLE with global coupling, the results of our study might find applications far beyond the field of physical chemistry. They could be viewed in the context of recent interest in emergence of synchrony in large populations of interacting oscillators (see, e.g., Refs. 20 and 21) and general aspects of self-organization in nonequilibrium reaction–diffusion systems. It should also be remarked that the effects of global coupling can lead to interesting complex behavior in a different class of systems, i.e., in excitable and bistable media.[22]

The authors acknowledge stimulating discussions with L. Kramer and would like to thank S. Wasle for the preparation of drawings. Financial support of the Thyssen Foundation and Deutche Forschungsgemeinschaft is gratefully acknowledged.

[1] F. Schueth, B. E. Henry, and L. D. Schmidt, Rev. Adv. Catal. **39**, 51 (1993).
[2] G. Ertl, Adv. Catal. **37**, 213 (1990().
[3] R. Imbihl, Progr. Surf. Sci. **44**, 185 (1993).

[4] S. Jakubith, H. H. Rotermund, W. Engel, A. von Oertzen, and G. Ertl, Phys. Rev. Lett. **65**, 3013 (1990).
[5] G. Veser and R. Imbihl, J. Chem. Phys. **96**, 7155 (1992).
[6] G. Veser, F. Mertens, A. S. Mikhailov, and R. Imbihl, Phys. Rev. Lett. **77**, 975 (1993).
[7] F. Mertens, R. Imbihl, and A. Mikhailov, J. Chem. Phys. **99**, 8668 (1993).
[8] Y. Kuramoto, *Chemical Oscillations, Waves and Turbulence* (Springer, Berlin, 1984).
[9] A. S. Mikhailov and A. Yu. Loskutov, *Foundations of Synergetics II. Complex Patterns* (Springer, Berlin, 1991).
[10] P. Coullet, L. Gill, and J. Lega, Phys. Rev. Lett. **62**, 1619 (1989).
[11] Th. Bohr, A. W. Petersen, and M. H. Jensen, Phys. Rev. A **42**, 3226 (1990).
[12] B. I. Shraiman, A. Pumir, W. van Saarlos, P. C. Hohenberg, H. Chate, and M. Holen, Physica D **57**, 241 (1992).
[13] A. Weber, L. Kramer, I. S. Aranson, and L. Aranson, Physica D **61**, 279 (1992).
[14] A. Newell, Lect. Appl. Math. **15**, 157 (1974).
[15] P. Coullet and K. Emilsson, Physica A **88**, 190 (1992); Physica D **61**, 119 (1992).
[16] H. Levine and X. Zou, Phys. Rev. Lett. **69**, 3013 (1990).
[17] N. Bekki and K. Nozaki, Phys. Lett. A **110**, 133 (1985).
[18] I. Aranson, A. Weber, and L. Kramer, Phys. Rev. Lett. **72**, 2316 (1994).
[19] G. Veser, F. Esch, and R. Imbihl, Catal. Lett. **13**, 371 (1992).
[20] H. Hakim and W.-J. Rappel, Phys. Rev. A **46**, 7347 (1992).
[21] M. Tsodyks, I. Mitkov, and H. Sompolinsky, Phys. Rev. Lett. **71**, 1280 (1993).
[22] U. Middya, D. Luss, and M. Sheintuch, J. Chem. Phys. **100**, 3568 (1994).